

MODAL ANALYSIS OF ALUMINIUM PLATE FOR SHORT SPAN FOREST BRIDGE DESIGN

Khirwizam Md Hkhir¹ and Mohd Rizuwan Mamat²

¹Politeknik Ungku Omar, Ipoh, Perak

²Forestry Division, Forest Research Institute Malaysia (FRIM), Selangor

Abstract: Stream crossing is one of the components in forest road construction to protect water quality during timber harvesting operations. Proper management of this network allows the post harvesting activities in the way to manage the forest sustainably. Poor stream crossing design and improper installation lead to erosion and sedimentation that disconnect the accessibility to the harvesting area unless the bridge is repaired. The forest bridge usually is made of native log and left deteriorated at the end of the logging period. Therefore, this study focuses on a new concept of a bridge which emphasizes simplicity site installation and is capable of serving stream crossing at multiple sites. This study shows the short span forest bridge design for modal analyses by assessing dynamic properties of aluminium plate for light weight characteristic in portable bridge application. Comparison of natural frequencies and mode shapes for four boundary conditions show the capability of modal analysis to characterize the proposed design structure.

Keyword: aluminium, natural frequency, mode shape, exact solution, finite element analysis

1. Introduction

1.1 Forest Management

In Malaysia, under the Selective Management System (SMS) system, forest harvesting needs to comply with the standard operating procedure prescribed in the forest harvesting guideline (MTC 2007). Forest management is to ensure the supply of timber-based is economically sustainable with minimum impact on the environment. Harvesting operations by nature are a disruptive process that proper management will certainly not hinder ecological or environmental functions. Forest harvesting is currently being carried out at the remote area in the forest where ecological damage normally caused by forest road construction. Stream crossing is one of the components in forest road construction to protect water quality with a positive ecological and aesthetic result of harvesting operations.

During timber harvesting operation, the bridges are constructed temporarily using the native logs as a stringer and removed or left to deteriorate at the end of the use period (Taylor et al. 1995) as stated in the current logging road specification (Jabatan Perhutanan Semenanjung Malaysia 2013). Almost all timber species would allow usage less than three

years (Mamat and Ahmad 2020), and the service life could be extended (Chow 2018) with a good structure design and hardwood species selection. However, this condition is subjected to site-specific soil and climatic conditions (Forestry Training Centre Incorporated 2010). Timber bridge damage often occurs internally and leaves no visible signs of decay on the surface (Morison et al. 2002). Poor stream crossing structure design and improper construction lead to erosion of stream banks and also sedimentation which is caused by high velocity of water flow and eventually collapsing the bridge (Leete 2008).

Forest road network is generally constructed with a single lane and unpaved and exposed to the light vehicle at the early of the forest opening. However, these roads will be exposed to extensive usage during logging operations where the heavy vehicles are used for log transportation and maybe more than legal highway load. This road is typically used only for a short period with a prolonged usage cycle, and this leads the management to close these roads whenever there are no logging activities (Taylor et al. 1995). Practically Forestry Department (FD) will carry out post harvesting activities such as replanting, soil treatment and research at the logged over area (Mamat et al. 2019).

Typical in forestry application, light construction equipment is expected to be used with a minimum installation and removal process. The ability of a portable bridge to serve multiple installations makes them much more economically feasible than a single permanent bridge structure. Thus, the bridge must be designed to comply with the required safety aspect and related design code (Nor et al. 2010) that is capable of supporting the applied bearing load. Therefore, a new design of bridge structure should be developed to serve the multi sites stream crossing which considering cost-effective, easy for transportation, installation and dismantling.

1.2 Design of Forest Mobile Bridge

New bridge design with the modular system shows the trend to move from difficult and time consuming to simplicity at the site. The prefabrication concept could practically be applied for low-volume bridge construction and gives advantages for material efficiency aside from reducing cost and time (GangaRao and Zelina 1989). The modular bridge consists of the segmented bridge components that are assembled for stream crossing, or each segment could function as its own. The design of modular forest bridge with a lightweight material could be a dependable, low-maintenance bridge material capable of delivering high performance over the life of a bridge structure.

In reducing the weight of structures, material replacement is more effective and economical than structural modification (Abdollah and Hassan 2013). Combination of different materials in the bridge system would enable optimal use of materials to achieve reasonable stiffness, capacity, and also lowering the cost. Hybrid material offers an efficient arrangement of these materials where these lightweight beams that may be used in accelerated bridge construction, installation and dismantling could only be carried out by manpower. Three primary materials suggested for portable bridge constructions are timber, aluminium and fibre reinforced polymer (Mamat 2018).

In this study, aluminium has been chosen for significance contribution to design and construction (Goorts et al. 2017). Besides, characteristic of corrosion resistance and high strength-to-weight ratio make this material as an excellent alternative to traditional materials for the construction (Dey 2017). Furthermore, aluminium is also a ductile material where it can be extruded into complicated sections such as for fabricating lightweight roof structures and window frames generally smaller in size range compare to steel (Megson 2005). Abdollah and Hassan (2013) compare the impact energy absorption characteristics on aluminium alloy and high-strength steel. The test results showed that the impact energy absorption of aluminium alloy was higher than that of high-strength steel because of higher ductility. In bridge deck design, aluminum orthotropic deck shows a structurally strong, lightweight deck weighing comparable to the open-grid steel deck (Klaiber and Wipf 2000).

1.3 Modal Analysis of Forest Bridge

Modal analysis is the study of dynamic properties of the structure to determine the natural frequencies and the vibration mode shapes of a structure. The natural frequencies of a structure are the frequencies at which the structure naturally tends to vibrate if it is subjected to a disturbance (Hauksson 2005). This forced vibration method is capable of measuring the natural frequency (bending mode) of the structures (Wang et al. 2005) by the excitation of the bridge, measure of response, analysis of data. Determination of natural frequency is important since their relation to frequency content of forcing function has major influence on the bridge response (Madda and Kalyanshetti 2013).

Dynamic properties, such as natural frequencies and mode shapes have been found to effectively characterize the state of a structure. As a common rule, the frequency decreases as the stiffness of the system decreases (Cheng 2005). Higher mode shapes in the primary structure are often accompanied by smaller local deflections, depending upon input energy at the corresponding band (Smith 2004). The first, fourth, and sixth modes are identified as longitudinal bending modes. The second and fifth modes are torsional modes. The third mode is a transverse bending mode (Jawad 2010). Lowest natural frequencies will help the designer to improve the stability and safety of the tested structure. Besides, these natural frequencies will show the possibilities of the structure to have resonance phenomenon under vibration excitation. Mass and stiffness of the structure characteristic are the contributor to the natural frequency of the beam (Madda 2013).

Morison (2002) correlates the first bending mode frequency to the stiffness characteristics of the bridge stringers. Tirelli (2011) modeling the bridge mode shapes found that the measurement seems to be closer to “free-free” beam boundary condition. Applying free vibration analysis, the first natural frequencies and mode shapes for the T-beam bridge deck is 10.127 (Jawad 2010). The estimation of fundamental frequency for slab on girder bridges range from 1 to 10 Hz (Roeder 2002) while limit for vertical frequency (Hz) by AASHTO LRFD is less than 3.0 Hz (Dey 2017). The estimated vehicle natural frequency is between 2 to 5 Hz (Roeder 2002).

For a complex structural system the fundamental bending mode is not necessarily the first mode, as in the case of a simple beam. The increase in natural frequency of the

structure when the concrete deck was replaced with the FRP deck is approximately 45 % (Hag-Elsafi 2012). Improved construction materials can be more highly stressed under static loads leads to more slender structures, smaller cross sectional dimensions and greater spans. As a consequence, stiffness and mass decrease leading to smaller natural frequencies resulting in more sensitivity to dynamic loads. Excessive vibrations can be caused by resonance when the natural frequencies often coincide with the dominant frequencies of the induced load (Hauksson 2005). Roover (2003) obtained the first natural frequency 10.5 Hz which is high enough for the bridge that concluded the uncertainty of the deformation due to the modular connection systems.

2. Methodology

Plate structures are one of the most important element components of structures used in civil, mechanical, marine and aerospace engineering. The application of multi-span rectangular plates has made the vibration analysis essential for minimizing the vibratory response and stress excited by dynamic loads (Cheung 2000). This study applied the study on homogeneous Kirchhoff plate (Catania 2011) to analyze lateral vibrations on the aluminium plate.

Various analytical and numerical methods have been developed to investigate the vibration behavior of plates, Rayleigh method (Biancolini 2005), where in this paper proposed a simplified method to evaluate the natural frequencies of plate. The method starts from a general expression of the fundamental frequency of a plate, suggested by Hearmon (Chiba 2003) and based on three coefficients that take into account the constraint condition by means of a simple numerical procedure that uses a particular formulation of the Rayleigh method.

The approach of this study is laboratory experimental and theoretically for the case of aluminium plate. The material properties of the aluminium taken for this study are 70 GPa Young Modulus, Density is 2710 kg/m³ and 0.346 for Poisson ratio. The theoretical using exact solution method for natural frequencies for plate case while the experiment both program dBFA Suite and ME'scope. Both approaches generate natural frequencies and mode shapes for comparison.

2.1 Exact Solution of Plate

Equation (1) is known as the *characteristic equation* of the system. For an n -degree-of-freedom system, both M and K are $n \times n$ matrices. It follows that the characteristic equation has n roots for ω^2 . For physically realizable systems, these n roots are all non-negative and they yield the n natural frequencies $\omega_1, \omega_2, \dots, \omega_n$ of the system.

$$\det[\omega^2 M - K] = 0 \quad (1)$$

One of the methods to determine the natural frequencies is using Exact Solution method. Below is the equation of dynamic equilibrium with biharmonic operator (D) for natural frequencies of a plate. A system of reference with axes x and y contained in the mid plane

of the plate is stated that assumed not to deform during bending (called a *neutral plane* or *surface*). The force distribution acting on the plane is then $f_z(x, y, t)$ and the displacement is $u_z(x, y, t)$. Neglecting the rotational inertia of the cross section and shear deformation, the following dynamic equilibrium equation can be obtained

$$\frac{\rho h}{D} \frac{\partial^2 u_z}{\partial t^2} + \frac{\partial^4 u_z}{\partial x^4} + 2 \frac{\partial^4 u_z}{\partial x^2 \partial y^2} + \frac{\partial^4 u_z}{\partial y^4} = \frac{f_z}{D} \quad (2)$$

where, $D = \frac{Eh^3}{12(1-\nu^2)}$ is the bending stiffness of the plate.

In the study of free vibration to determine natural frequency, the force $f_z(x, y, t)$ must be set to zero and equation (1) reduces to a homogeneous equation. Its solution can be expressed as the product of a function of the space coordinates by a function $u_z(x, y, t) = q(x, y)\omega(t)$, which is the two-dimensional. The function of time $\omega(t)$ that solves equation (1) is harmonic. Also, in this case function $q(x, y)$ can be regarded as a principal function and can be obtained from the equation

$$\omega^2 \frac{\rho h}{D} q(x, y) = \frac{\partial^4 q(x, y)}{\partial x^4} + 2 \frac{\partial^4 q(x, y)}{\partial x^2 \partial y^2} + \frac{\partial^4 q(x, y)}{\partial y^4} \quad (2a)$$

$$\left(\omega \sqrt{\frac{\rho h}{D}} \right)^2 q(x, y) = \frac{\partial^4 q(x, y)}{\partial x^4} + 2 \frac{\partial^4 q(x, y)}{\partial x^2 \partial y^2} + \frac{\partial^4 q(x, y)}{\partial y^4} \quad (2b)$$

$$\frac{\partial^4 q(x, y)}{\partial x^4} + 2 \frac{\partial^4 q(x, y)}{\partial x^2 \partial y^2} + \frac{\partial^4 q(x, y)}{\partial y^4} - \left(\omega \sqrt{\frac{\rho h}{D}} \right)^2 q(x, y) = 0 \quad (2c)$$

where ω is an undetermined constant. The substitution $Q(x) = e^{kx}$ leads to the general solution, since $\cosh a = (e^a + e^{-a})/2$, $\sinh a = (e^a - e^{-a})/2$

$$Q(x) = C_1 \cosh kx + C_2 \sinh kx + C_3 \cos kx + C_4 \sin kx \quad (3a)$$

$$Q(y) = C_5 \cosh ky + C_6 \sinh ky + C_7 \cos ky + C_8 \sin ky \quad (3b)$$

where $k = \left(\omega \sqrt{\frac{\rho h}{D}} \right)^{1/2}$ and $C_1, C_2, C_3, C_4, C_5, C_6, C_7$ & C_8 are as yet undetermined constant. These constants will determine by the boundary conditions.

Cheung (2000) applying three types of boundary conditions which are clamped support, simply support and free edge. This paper applied only 2 types of boundary condition which are Clamped and Free Edges. The clamped boundary condition referred to 1 edge clamp, 2 edges clamp and 4 edges clamp. The parameters to be set up before the experiment are the deflection, slope and bending moment.

Boundary Condition 1: Free Edges

No clamped along all axis

The boundary condition :

$$\text{Bending Moment} : \frac{\partial^2 Q(x)}{\partial x^2} = 0 \quad \text{at} \quad x = 0 \quad \& \quad x = l$$

$$\text{Shearing Force} : \frac{\partial^3 Q(x)}{\partial x^3} = 0 \quad \text{at} \quad x = 0 \quad \& \quad x = l$$

$$\text{Bending Moment} : \frac{\partial^2 Q(y)}{\partial y^2} = 0 \quad \text{at} \quad y = 0 \quad \& \quad y = l$$

$$\text{Shearing Force} : \frac{\partial^3 Q(y)}{\partial y^3} = 0 \quad \text{at} \quad y = 0 \quad \& \quad y = l$$

The natural frequency of the plate will be determined from the solution of

$$x \text{ \& } y \text{ along length of plate, } l \quad kl = \left(\omega \sqrt{\frac{\rho h}{D}} \right)^{1/2}$$

$$\omega = \left(\frac{k}{l} \right)^2 \sqrt{\frac{D}{\rho h}}$$

therefore,

$$\omega = k^2 \sqrt{\frac{D}{\rho l^4 h}} = k^2 \sqrt{\frac{Eh^2}{\rho l^4 (1-\nu^2)}} \text{ rad / sec}$$

Boundary Condition 2: 1 Edge Clamp

Clamped along x-axis only

The boundary condition :

$$\text{Deflections} : Q(x) = 0 \quad \text{at} \quad x = 0$$

$$\text{Slope} : \frac{\partial Q(x)}{\partial x} = 0 \quad \text{at} \quad x = 0$$

$$\text{Bending Moment} : \frac{\partial^2 Q(x)}{\partial x^2} = 0 \quad \text{at} \quad x = l$$

$$\text{Shearing Force} : \frac{\partial^3 Q(x)}{\partial x^3} = 0 \quad \text{at} \quad x = l$$

The natural frequency of the plate will be determined from the solution of,

$$\text{where } x \text{ along length of plate, } l \quad kl = \left(\omega \sqrt{\frac{\rho h}{D}} \right)^{1/2}$$

$$\omega = \left(\frac{k}{l} \right)^2 \sqrt{\frac{D}{\rho h}}$$

therefore,

$$\omega = k^2 \sqrt{\frac{D}{\rho l^4 h}} = k^2 \sqrt{\frac{Eh^2}{\rho l^4 (1-\nu^2)}} \text{ rad / sec}$$

Boundary Condition 3: 2 Edges Clamp

Clamped along 1 x-axis and 1 y-axis

The boundary condition :

$$\text{Deflections: } Q(x) = 0 \quad \text{at} \quad x = 0$$

$$\text{Slope} \quad : \quad \frac{\partial Q(x)}{\partial x} = 0 \quad \text{at} \quad x = 0$$

$$\text{Deflections: } Q(y) = 0 \quad \text{at} \quad y = 0$$

$$\text{Slope} \quad : \quad \frac{\partial Q(y)}{\partial x} = 0 \quad \text{at} \quad y = 0$$

The natural frequency of the plate will be determined from the solution of

$$x \text{ \& \& } y \text{ along length of plate, } l \quad kl = \left(\omega \sqrt{\frac{\rho h}{D}} \right)^{1/2}$$

$$\omega = \left(\frac{k}{l} \right)^2 \sqrt{\frac{D}{\rho h}}$$

therefore,

$$\omega = k^2 \sqrt{\frac{D}{\rho l^4 h}} = k^2 \sqrt{\frac{Eh^2}{\rho l^4 (1-\nu^2)}} \text{ rad / sec}$$

Boundary Condition 4: 4 Edges Clamp

Clamped along all axis

The boundary condition :

$$\text{Deflections: } Q(x) = 0 \quad \text{at} \quad x = 0 \quad \& \quad x = l$$

$$\text{Slope} \quad : \quad \frac{\partial Q(x)}{\partial x} = 0 \quad \text{at} \quad x = 0 \quad \& \quad x = l$$

$$\text{Deflections: } Q(y) = 0 \quad \text{at} \quad y = 0 \quad \& \quad y = l$$

$$\text{Slope} \quad : \quad \frac{\partial Q(y)}{\partial y} = 0 \quad \text{at} \quad y = 0 \quad \& \quad y = l$$

The natural frequency of the plate will be determined from the solution of

$$x \text{ \& \& } y \text{ along length of plate, } l \quad kl = \left(\omega \sqrt{\frac{\rho h}{D}} \right)^{1/2}$$

$$\omega = \left(\frac{k}{l} \right)^2 \sqrt{\frac{D}{\rho h}}$$

therefore,

$$\omega = k^2 \sqrt{\frac{D}{\rho l^4 h}} = k^2 \sqrt{\frac{Eh^2}{\rho l^4 (1-\nu^2)}} \text{ rad / sec}$$

The value of k^2 for all boundary condition (Harris and Piersol 2002) are as Table 1

Table 1: Value of k^2 for all boundary condition

Boundary Condition	Value of k^2 for mode			
	1	2	3	4
1 edge clamp	1.01	2.47	6.20	7.94
2 edges clamp	2.01	6.96	7.74	13.89
4 edges clamp	10.40	21.21	31.29	38.04
Free Edges	4.07	5.94	6.91	10.39

2.2 Modal Experiment of Plate

In this study the result obtained from the experiment and to be compared to the theoretical result. To undertake the experiment, an aluminum plate of 300 mm x 30 mm x 2 mm (Figure 1) dimensions was prepared and marked on every 50 mm on X and Y axes. Then the points will be numbered consecutively.

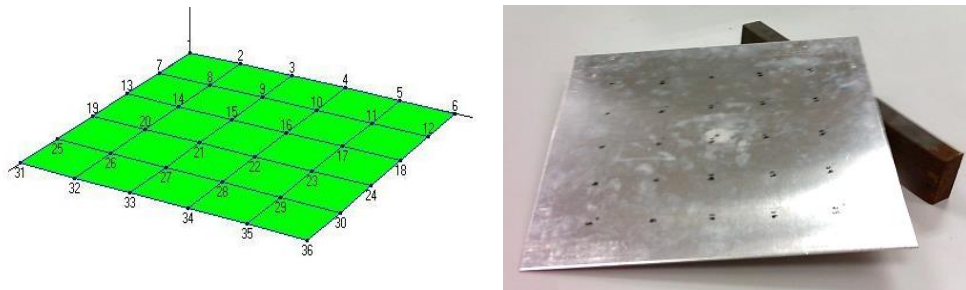


Figure 1: Aluminum Plate Specimen

2.3 Experimental boundary condition

In preparing the experiment, the plate was placed at the clamp-instrument for the clamped condition case or to be hanging for free constraint case (Figure 2). The main instruments for the experiment were a hammer, a transducer and a 4-Channel FFT analyzer for excitation, measurement and time to frequency domain processing respectively. ME'Scope software was used for signal post processing for modal analysis. The source for the excitation signal would depend on the type of taken test. In our case as impact testing, this allowed the real-time analysis of transient phenomena.

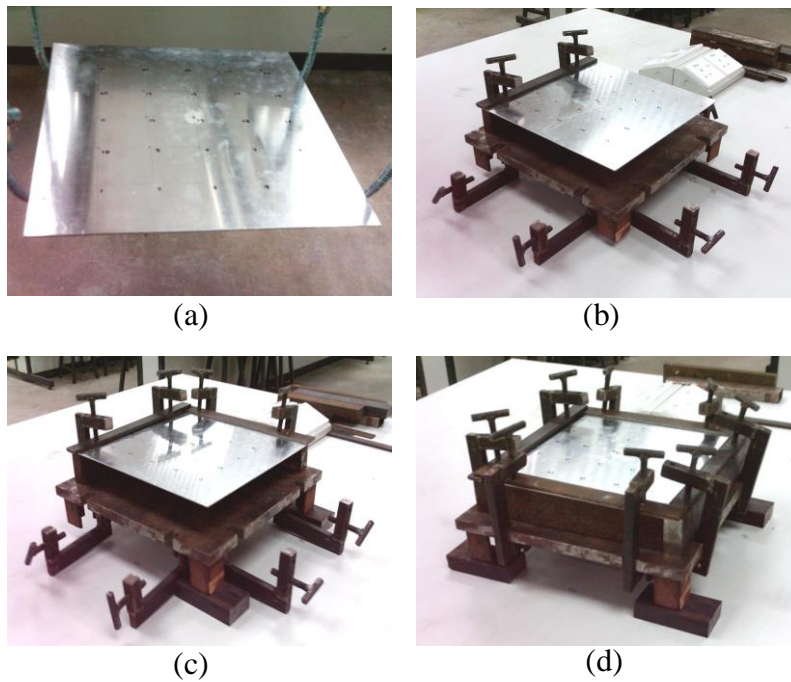


Figure 2 : a) free edges, b)1 edge clamp, c)2 edges clamp, d)4 edges clamp

The plate was excited into vibration by using an impact hammer (Figure 3) with 0.01138 V/PU sensitivity and 0.15 Hz filtering and the transducer detected the magnitude of the force impacted. The marked points on the specimen will be impacted to get the frequency response. The accelerometer (Figure 3) absorbs the knocking vibration and processes the signal into magnitude and frequency. The signal then transferred to the 4-Channel FFT Analyzer (Figure 3) to convert the vibration signal into Frequency Response Function (FRF).

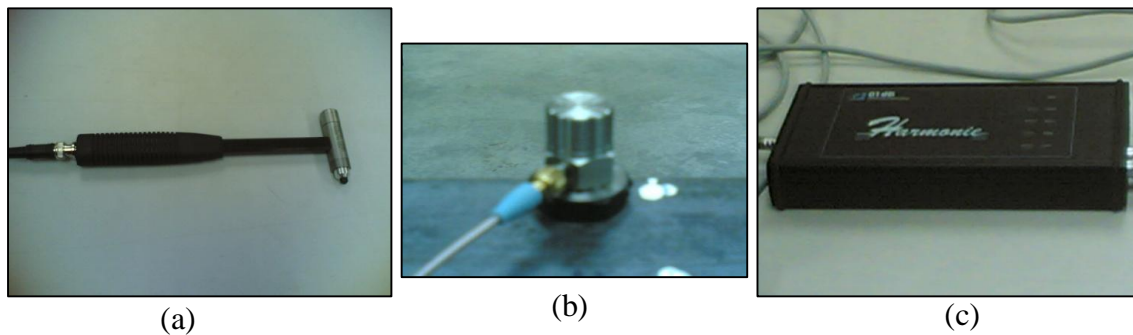


Figure 3: a) Impact hammer, b)Accelerometer, c) FFT Analyzer

In this case, the accelerometers type ACC 3715 with 0.101 V/PU sensitivity and 0.15 Hz filtering which located at point 13 (center of the specimen) stucked with glue. 4-Channel

FFT Analyzer measures the various signals developed by the transducer to get the magnitudes of the excitation force and responses. Like the voltmeter, this part is connected to dbRTA software and uses Spectrum (Fourier) Analyzers function to get the Frequency Response Function (FRF) and Coherence Function (Figure 4). Once the impact hammer excites the plate, the dbRTA software gives the frequency response function (FRF) for first time excitation at every point. When the second time excitation was applied, the coherence function was displayed as our reference. The measurements are considered being of reasonable quality if the coherence displays excess of unity and the magnitude of natural frequencies are extracted from the FRF

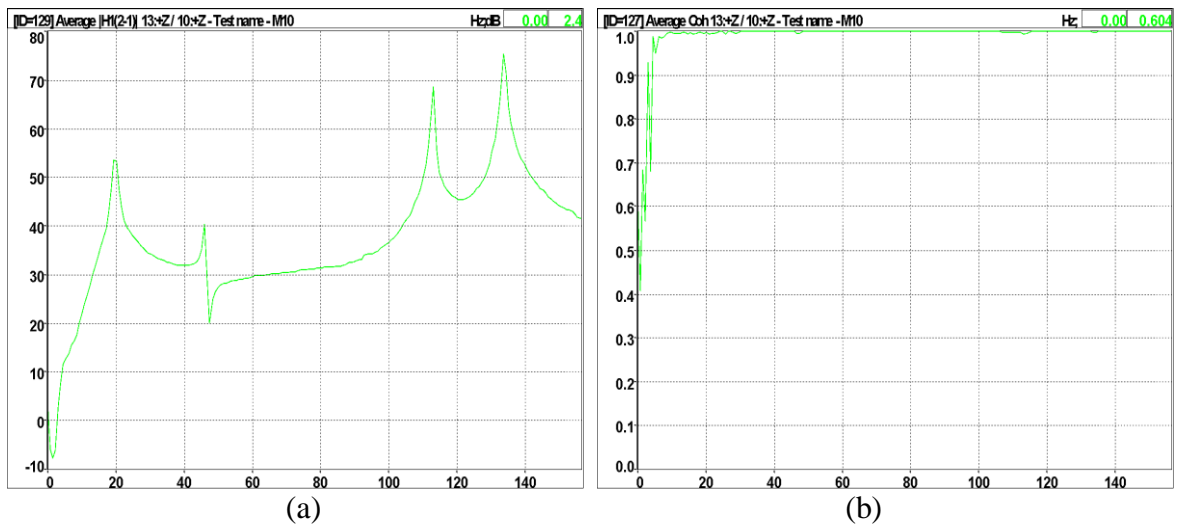


Figure 4: a) Frequency Response Function (FRF), b) Coherence Function

3. Result

3.1 Natural Frequency Comparison

The comparison between theoretical and experimental completed with first four natural frequencies and the mode shapes. The analyses were carried out with 4 cases of boundary condition which were 1 edge clamp, 2 edges clamp, 4 edges clamp and free edges. Comparison natural frequencies for theoretical and experimental are as in Table 2. The mode shapes for free edges, 1 edge clamp, 2 edges clamp and 4 edges clamp are as in Figure 5, Figure 6, Figure 7 and Figure 8 consecutively.

Table 2: Natural frequencies for all boundary condition

Boundary Condition	Mode Shape	Theory (Hz)	Experiment (Hz)	Error (%)
Free Edges	1st	77.97	78.1	0.17
	2nd	113.8	105	-7.73
	3rd	132.38	136	2.73
	4th	199.06	177	-11.08
1 Edge Clamp	1st	19.35	18.7	-3.36
	2nd	47.32	46.5	-1.73
	3rd	118.78	114	-4.02
	4th	152.12	133	-12.57
2 Edges Clamp	1st	38.51	37.5	-2.62
	2nd	133.34	131	-1.75
	3rd	148.29	148	-0.2
	4th	266.11	266	-0.04
4 Edges Clamp	1st	199.25	200	0.38
	2nd	406.35	394	-3.04
	3rd	599.47	594	-0.91
	4th	728.79	697	-4.36

The comparison result shows that the overall error between both method is less than 5 %.

3.2 Experimental Mode Shape

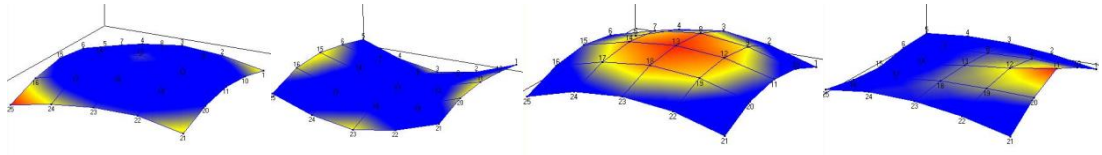


Figure 5: Free edges

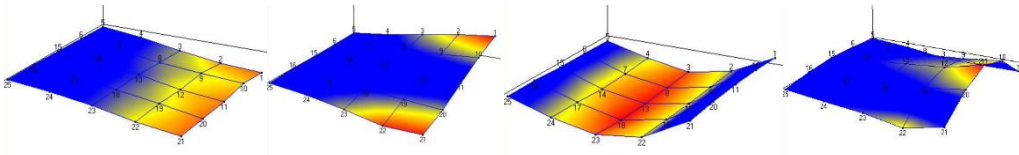


Figure 6: 1 Edge clamp

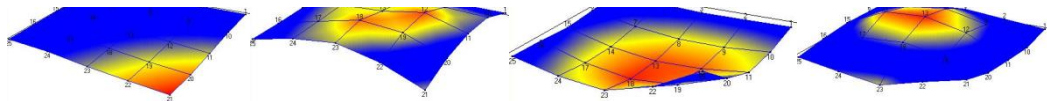


Figure 7: 2 Edges clamp

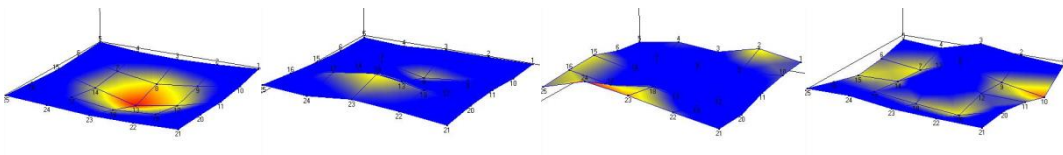


Figure 8: 4 Edges clamp

4. Discussion

Figure 9 shows the comparison of natural frequencies and mode shapes for four types of boundary conditions which are Free Edges, 1 Side Clamp, 2 Sides Clamp and 4 Sides Clamp. The natural frequencies show an increase with the increased number of mode shapes. The structure deflection is always smaller at the higher mode shapes (Smith 2004). Higher clamps show higher frequencies at different mode shapes. This is true to Cheng (2005) that mention the frequency decreases as the stiffness of the system decreases.

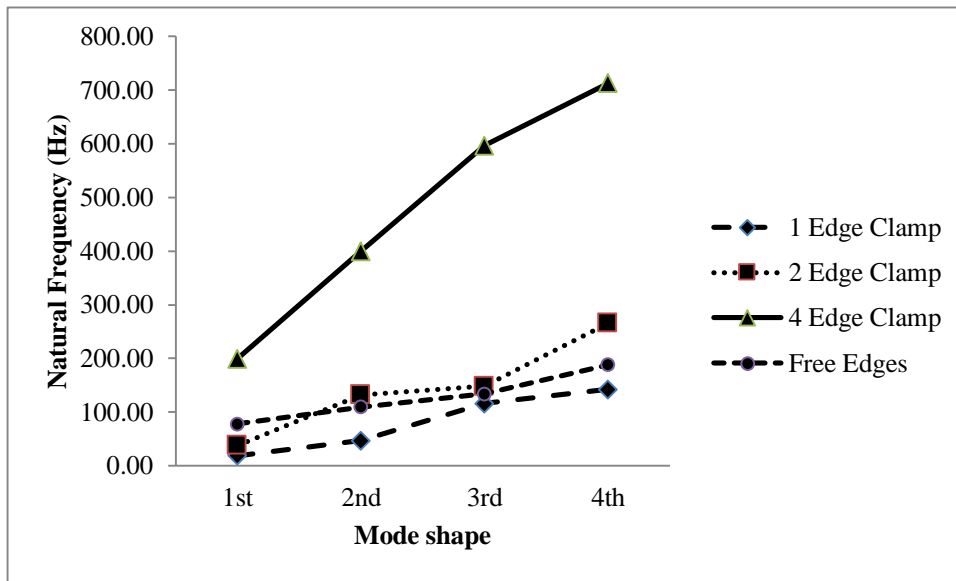


Figure 9: Natural frequencies for all mode shapes

The slope information for linear trend lines of all mode shapes for all boundary conditions shows that an increase of natural frequencies from free edges, single clamp, 2 edges clamp and the highest is 4 edges clamps (Figure 10).

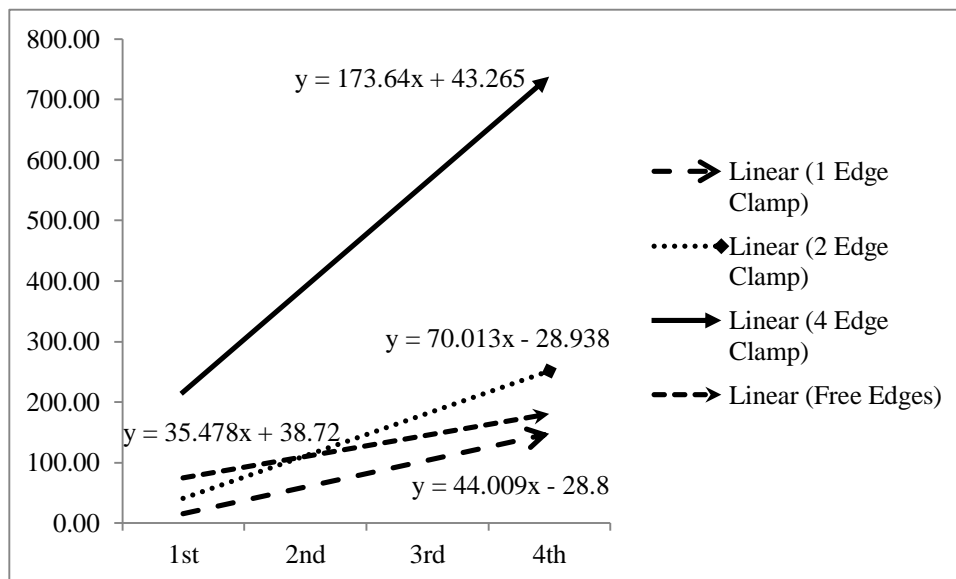


Figure 10: Linear trend lines for all boundary conditions

The slope shows that the 4 edges clamp of boundary condition contributes the highest stiffness and generates lowest deflection of the experimental model.

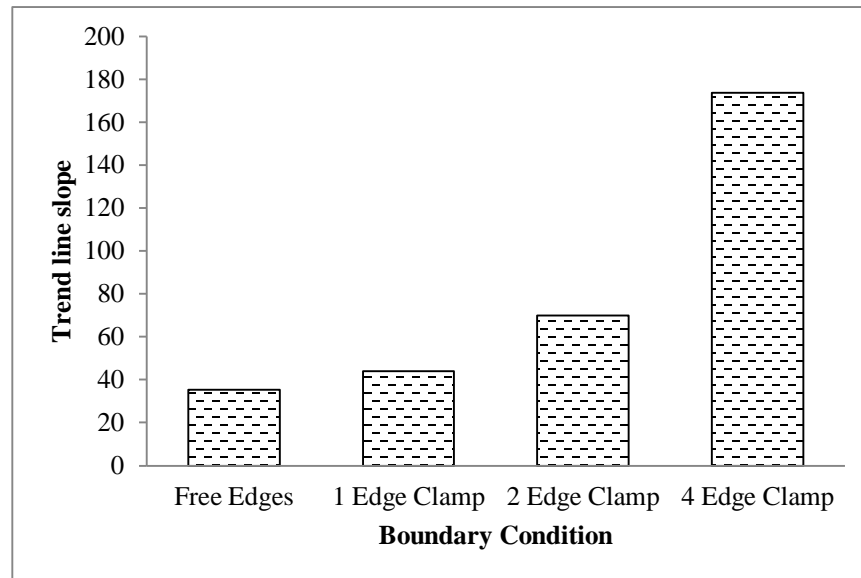


Figure 11: Trend line slope for all boundary conditions

In the bridge design application, the natural frequency of simply supported beam or bridge of uniform section depends only on the mass and stiffness of the structure (Madda 2013). The first, fourth, and sixth modes are identified as longitudinal bending modes, the second and fifth modes are torsional modes and the third mode is a transverse bending mode (Jawad 2010). The first mode shape gives the least frequency and maximum time period (Madda 2013), these dynamic properties could be used to be the first the modal analysis in designing the modular and portable bridge.

In this case study, the first natural frequency and mode shape for experimental considering “free-free” boundary condition (Tirelli 2011) is 78.10Hz. Practically, this frequency is compared to the vibration excitation as such the vehicle's natural frequency ranges 2 to 5 Hz (Roeder 2002). The proposed bridge would not coincide with the induced frequencies in order to avoid the possibilities to have resonance phenomenon.

5. Conclusion

Dynamic properties which are natural frequencies and mode shapes capable of characterizing the stiffness of Aluminium plate with 4 boundary conditions. The higher slope of mode shape linear trend lines shows higher stiffness of boundary condition applied to the Aluminium plate which will contribute to smaller amplitude of deflection for all boundary conditions. Therefore, analyzing the first mode shape important in designing the portable bridge system where this first mode shapes and natural frequency value shows that the stiffness of the bridge deck structure in order to avoid the resonance that can cause a magnification of the dynamic response which can lead to structural instability, overstressing or fatigue failure of materials.

References

- Abdollah, M. F. and Hassan, R. (2013). "Preliminary design of side door impact beam for passenger cars using aluminium alloy." *Journal of Mechanical Engineering and Technology*, 5(1), 11–18.
- Biancolini, M. E., Brutti, C., and Reccia, L. (2005). "Approximate solution for free vibrations of thin rectangular plates." *Journal of Sound and Vibration*, 288(1-2), 321–34422110.1016/j.jsv.2005.01.005.
- Catania, G. and Sorrentino, S. (2011). "Dynamic analysis of railway bridges by means of the 223 spectral method." *Conference Proceedings of the Society for Experimental Mechanics Series 7*, T. Proulx, ed., The Society for Experimental Mechanics, Inc. Springer. 21–30. <https://doi.org/10.1007/978-1-4419-9316-8>.
- Cheng, L. (2005). "Development of a steel-free frp-concrete slab-on-girder modular bridge system." Ph.D. thesis, UNIVERSITY OF CALIFORNIA,, SAN DIEGO.
- Cheung, Y. K. and Zhou, D. (2000). "Dynamic analysis of the bentley creek bridge with FRP deck." *Thin-Walled Structures*, 37(4), 305–331 [https://doi.org/10.1016/S0263-8231\(00\)00015-X](https://doi.org/10.1016/S0263-8231(00)00015-X).
- Chiba, M. and Sugimoto, T. (2003). "Vibration characteristics of a cantilever plate with attached spring–mass system." *Journal of Sound and Vibration*, 260.
- Chow, B. (2018). *Engineering Manual*. Ministry of Forests, Lands, Natural Resource Operation and Rural Development (MFLNRO).
- Dey, P., N. S. W. S. (2017). "Evaluation of design guidelines for the serviceability assessment of aluminum pedestrian bridges." *Engineering Structures*, 22(1), 040161091 – 0401610915. [https://doi.org/10.1061/\(ASCE\)BE.1943-5592.0000983](https://doi.org/10.1061/(ASCE)BE.1943-5592.0000983).
- Forestry Training Centre Incorporated (2010). *Forest road engineering*. Forestry Handbook. Forestry Training Centre Incorporated, New York, NY.
- GangaRao, H. V. S. and Zelina, T. R. (1989). "Development of economical low-volume road bridges." *Journal of Structural Engineering*, 114(9), 1941–1961.
- Goorts, K., Ashasi-Sorkhabi, A., and Narasimhan, S. (2017). "Deployable active mass dampers for vibration mitigation in lightweight bridges." *Journal of Structural Engineering*, 143(12), 16.
- Harris, C. and Piersol, A. (2002). *Harris' Shock and Vibration Handbook*. McGraw-Hill, New245York, NY 10121-2298.

- Hauksson, F. (2005). "Dynamic behaviour of footbridges subjected to pedestrian-induced vibrations." M.S. thesis, LUND University, SE-221 00 Lund, Sweden, <<http://www.byggmek.lth.se>>.
- Jabatan Perhutanan Semenanjung Malaysia (2013). *Garis Panduan Jalan Hutan 2010*. Jabatan Perhutanan Semenanjung Malaysia (JPSM). pindaan 2013.
- Jawad, D. A. M. and Mohamad-Ali, A. A. K. (2010). "Analysis of the dynamic behaviour of t-beam bridge decks due to heavyweight vehicles." *Emirates Journal for Engineering Research*, 15(2),29–39.
- Klaiber, F. and Wipf, T. (2000). *Bridge engineering handbook*. CRC Press, Boca Raton.
- Leete, R. (2008). *Malaysia Sustainable Community: Forest Management in Sabah*. United Nations Development Programme (UNDP), Kuala Lumpur, Malaysia.
- Madda, S. and Kalyanshetti, M. G. (2013). "Dynamic analysis of t-beam bridge super structure." *International Journal of Civil and Structural Engineering*, 3(3), 495–504 <https://doi.org/10.6088/ijcser.201203013045>.
- Mamat, M. R. (2018). "Design of modular mobile hybrid timber bridge reinforced with carbon fiber reinforced polymer (CFRP)." M.S. thesis, University Teknologi MARA (UiTM), Shah Alam, Selangor, Malaysia.
- Mamat, M. R. and Ahmad, W. M. S. W. (2020). "Connector design selection for modular forest bridge using finite element analysis." *International Conference on Architecture and Civil Engineering 2019*, M. Awang and M. R. M. M. Fared, eds., Springer Nature Singapore Pte Ltd., Lecture Notes in Civil Engineering (LNCE), 169–174.
- Mamat, M. R., Hashim, M. H. M., Ahmad, W. M. S. W., and H., A. (2019). "Static stress analysis of girder cross section for mobile forest bridge." *International Journal for Research in Engineering Application and Management (IJREAM)*, 4(12), 401–407.
- Megson, T. H. G. (2005). *Structural and Stress Analysis*. Elsevier Butterworth-Heinemann, Burlington, MA 01803.
- Morison, A., Karsen, C. D. V., Evensen, H. A., Ligon, J. B., Erickson, J. R., Ross, R. J., and Forsman, J. W. (2002). "Timber bridge evaluation: A global nondestructive approach using impact generated FRFs." *20th International Modal Analysis Conference (IMAC2002)*, Los Angeles, CA, 1567–1573. February 4-7.
- MTC (2007). *Malaysia: Sustainable Forest Management*. Malaysian Timber Council.

- Nor, N. M., Devarase, V., Yahya, M. A., Sojipto, S., and Osmi, S. K. C. (2010). "Fiber reinforced polymer (FRP) portable bridge: Modeling and simulation." *European Journal of Scientific Research*, 44(3), 437–448.
- Roeder, C. W., Barth, K., and Bergman, A. (2002). "Improved live load deflection criteria for steel bridges." *Technical Report NCHRP Web Document 46 (Project 20-7[133])*, American Association of State Highway and Transportation Officials (AASHTO).
- Roover, C. D., Vantomme, J., Wastiels, J., Croes, K., Taerwe, L., and Blontrock, H. (2003). "Modular pedestrian bridge with concrete deck and IPC truss girder." *Engineering Structures*, 25(4), 449–459 [https://doi.org/10.1016/S0141-0296\(02\)00185-2](https://doi.org/10.1016/S0141-0296(02)00185-2).
- Smith, K. and Shust, W. (2004). "Bounding natural frequencies in structures i: Gross geometry, material and boundary conditions." *Proceedings of the IMAC-XXII Conference and Exposition on Structural Dynamics*, Dearborn, Michigan., Society for Experimental Mechanics (SEM).
- Taylor, S. E., Ritter, M. A., and Murphy, G. L. (1995). "Portable glulam timber bridge design for low-volume forest road." *Proc., 6th International conference on low-volume roads*, National Academy of Sciences, Minneapolis, Minnesota, Transportation Research Board, 328–338.
- Tirelli, D. (2011). "Modal analysis of small and medium structures by fast impact hammer testing method." *Technical Report EUR 24964 EN - 2011*, Joint Research Centre, TP480 21027 Ispra(VA), Italy.
- Wang, X., Ross, R. J., Hunt, M. O., Erickson, J. R., and Forsman, J. W. (2005). "Low frequency vibration approach for assessing performance of wood floor systems." *Wood and Fiber Science*, 37(3), 371–378.